Minimal Dark Matter Freeze-in with Low Reheating Temperatures (Implications for Direct Detection)

Barmak Shams Es Haghi

Weinberg Institute for Theoretical Physics
UT Austin

Kimberly K. Boddy, Katherine Freese, Gabriele Montefalcone

arXiv:2405.06226

Mitchell Conference 2024
Texas A&M

May 23, 2024

Evidence for Dark Matter from all scales: Gravitational Interaction

Rotation Curves of Galaxies

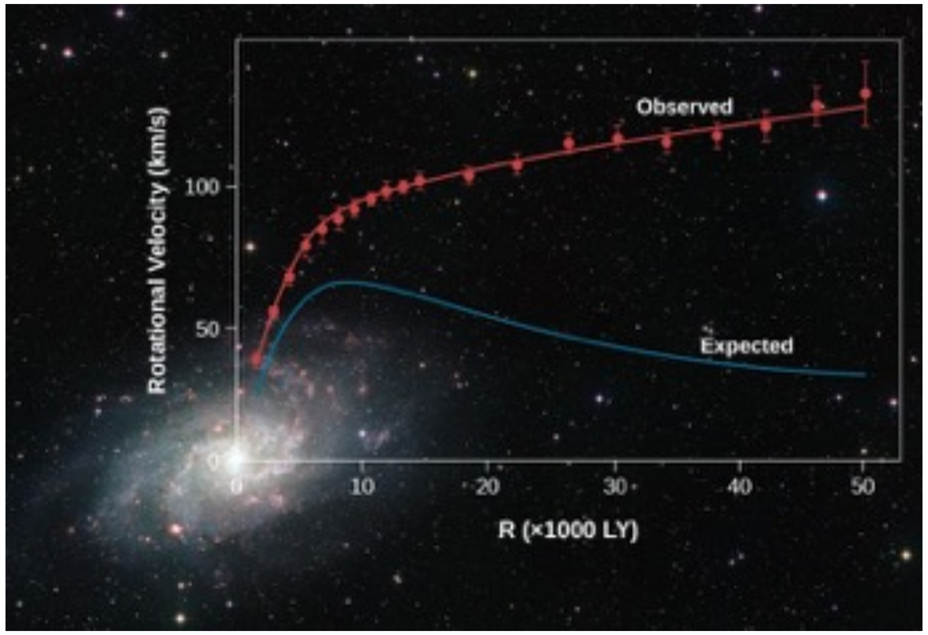

Gravitational Lensing

Structure Formation

Cosmic Microwave Background (CMB)

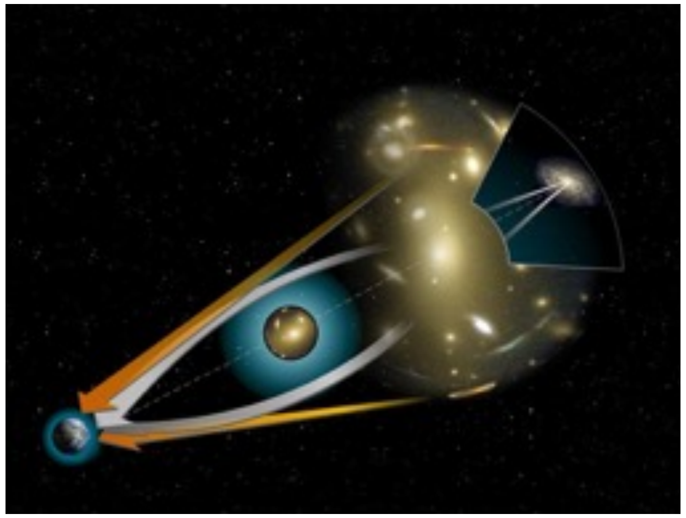

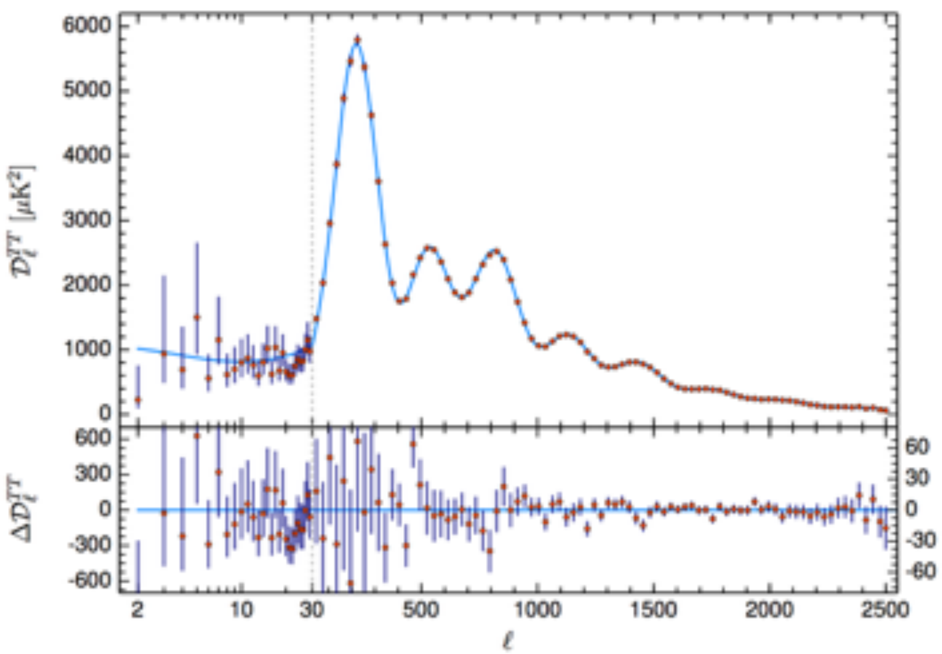

Nature of Dark Matter?

our knowledge is limited:
DM can be explained by candidates with a mass range spanning over 90 orders of magnitude.
each model can only be partially constrained.

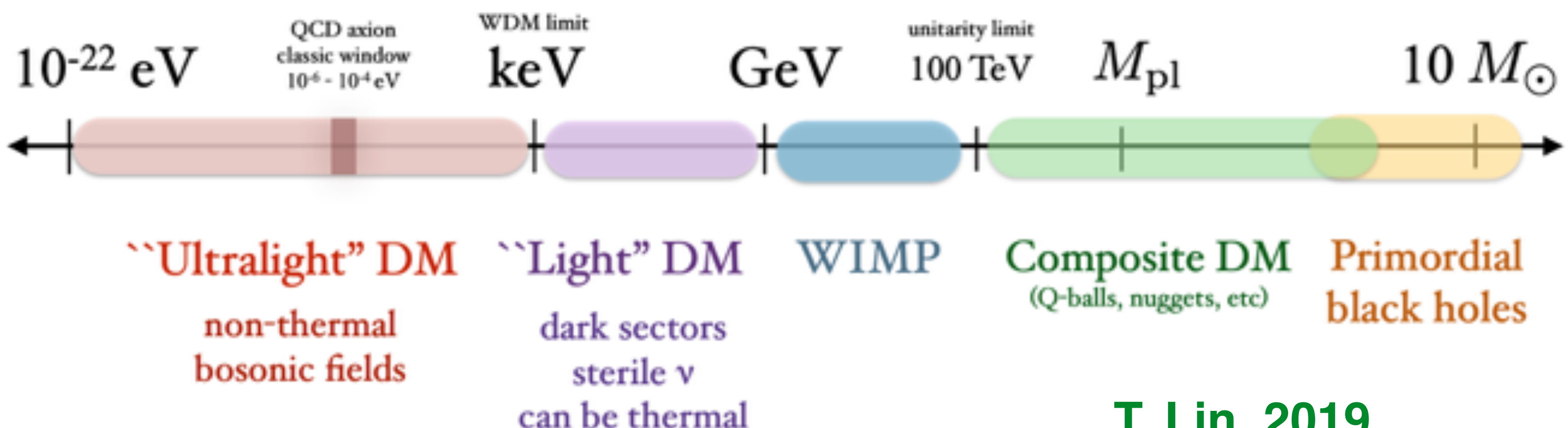

T. Lin, 2019

Ultimate goal:
Direct detection of DM through non-gravitational interactions!

A well-studied apronach to produce DM:
through interaction with the Standard Model **thermal bath.**

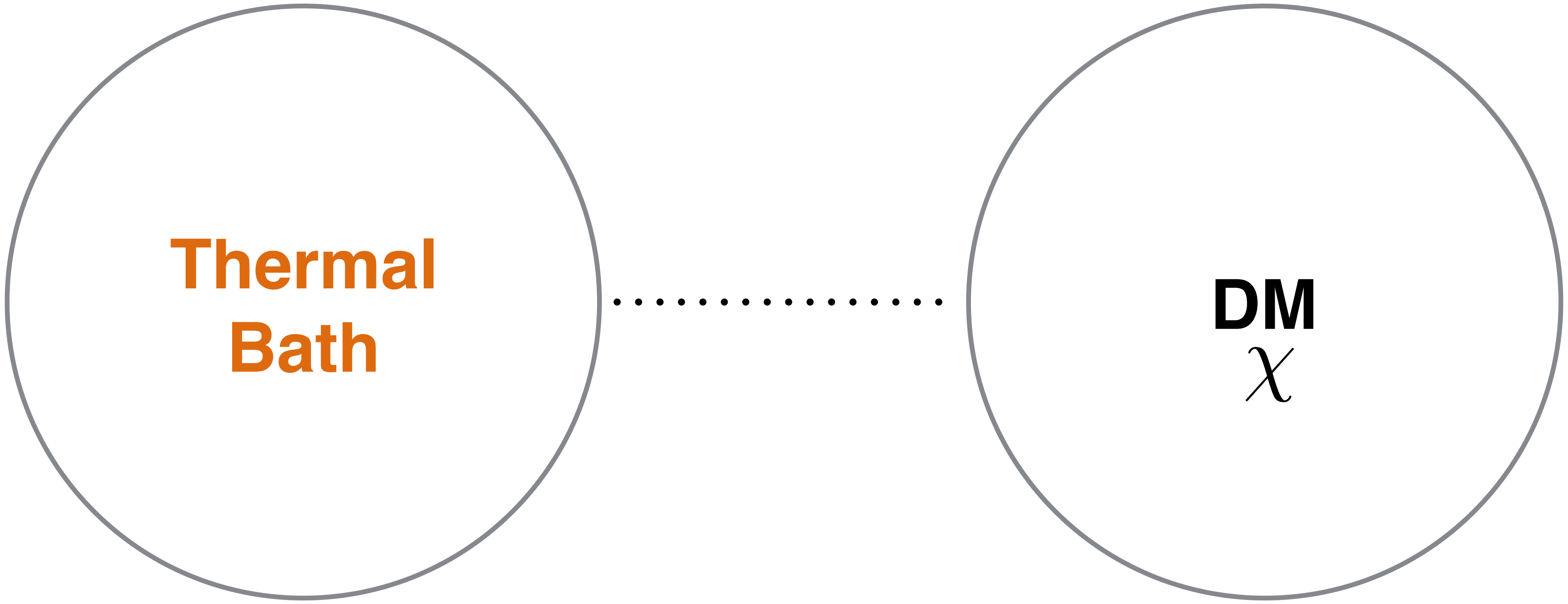

depending on the interaction:
DM abundance is mainly established by
freeze-out or **freeze-in** mechanisms.

Freeze-out:

$$\dot{n}_\chi + 3Hn_\chi = -\langle\sigma v\rangle \left(n_\chi^2 - n_{\chi,\mathrm{eq}}^2\right)$$

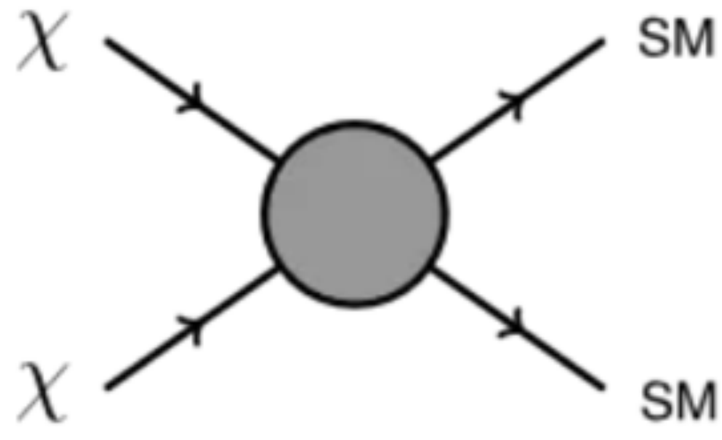

Due to thermalization:
no dependence on the initial temperature of the bath

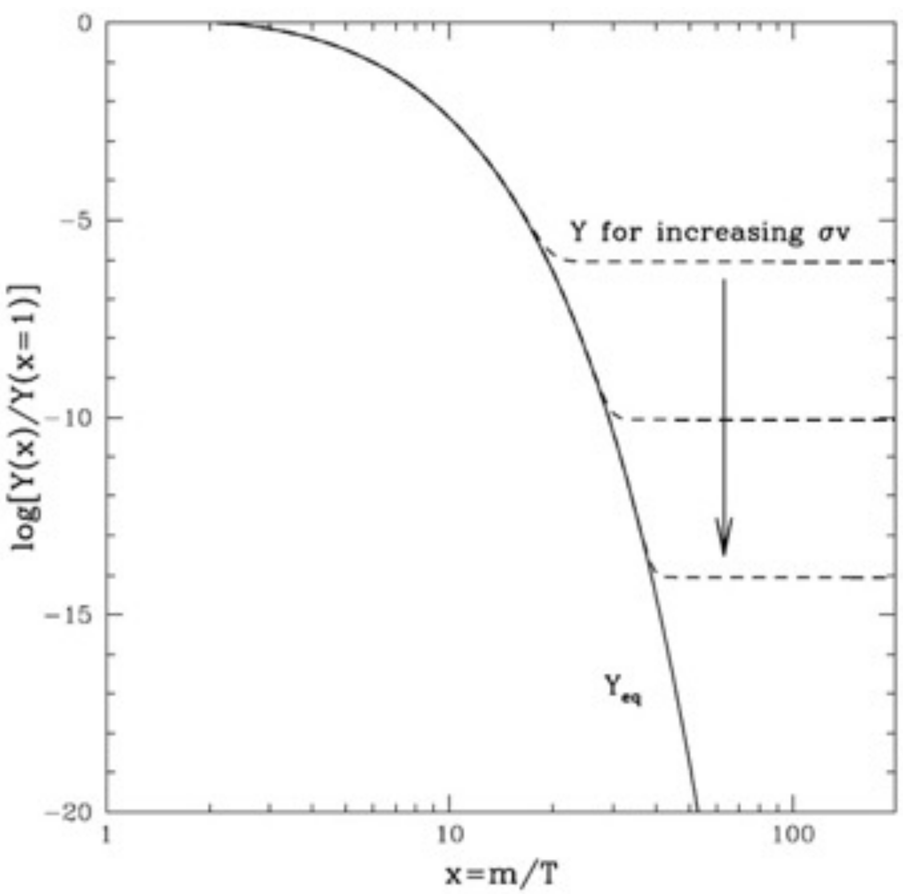

Example:WIMPs

weak-scale couplings, weak scale mass

WIMPs: benchmark targets for direct detection experiments

Nuclear recoil

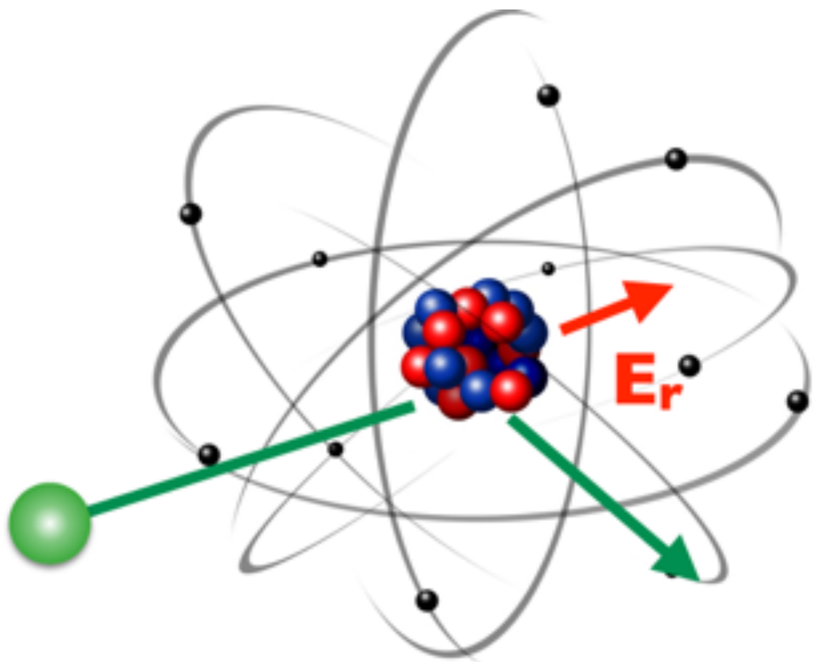

image credit: Carmen Carmona

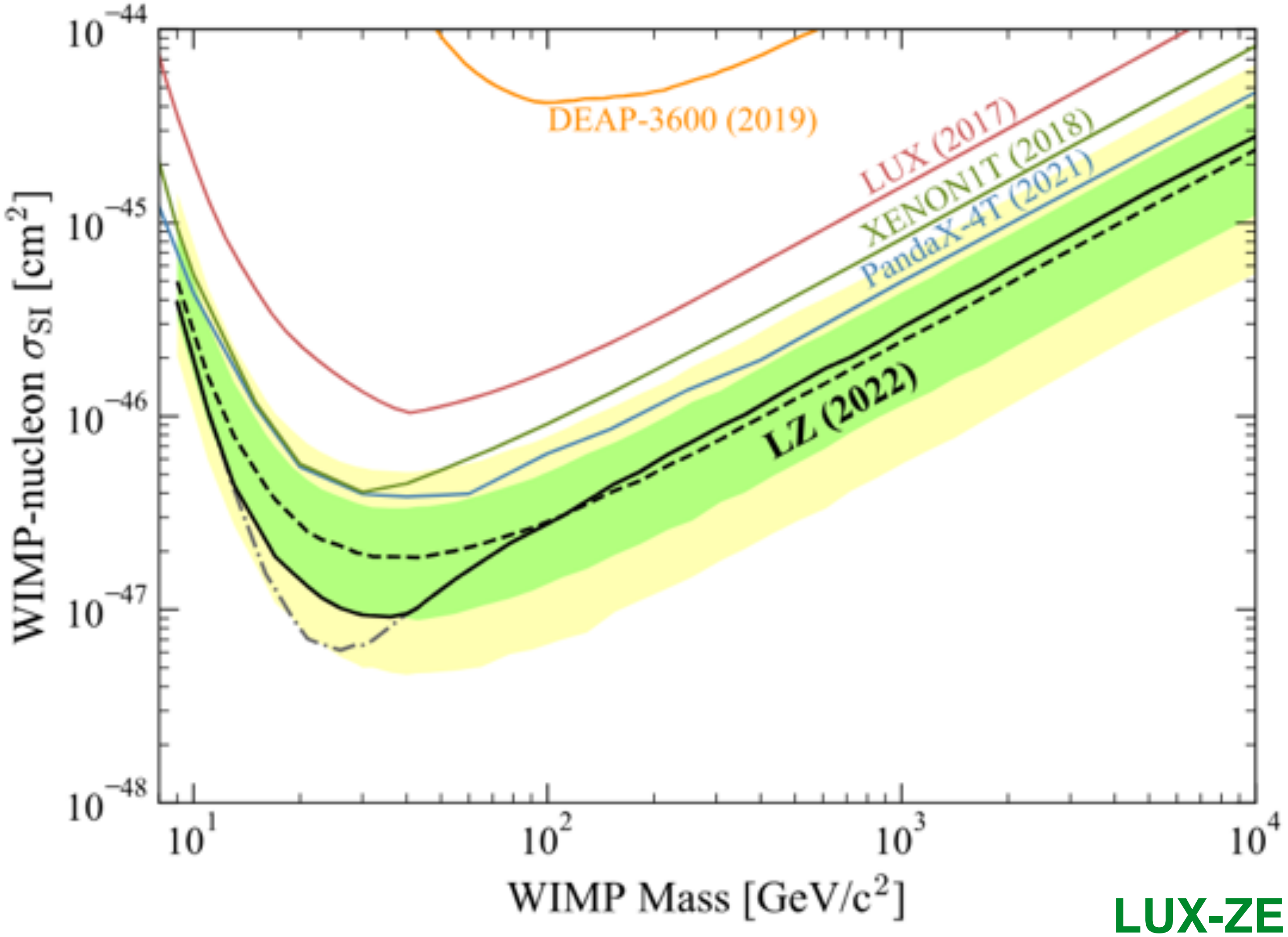

DM signal: a recoil rate that exceeds the detector-internal background

multi-ton-scale target masses

a clear path for even larger detectors to reach the neutrino fog

LUX-ZEPLIN (LZ) Experiment, 2022

Direct detection of Sub-GeV DM:

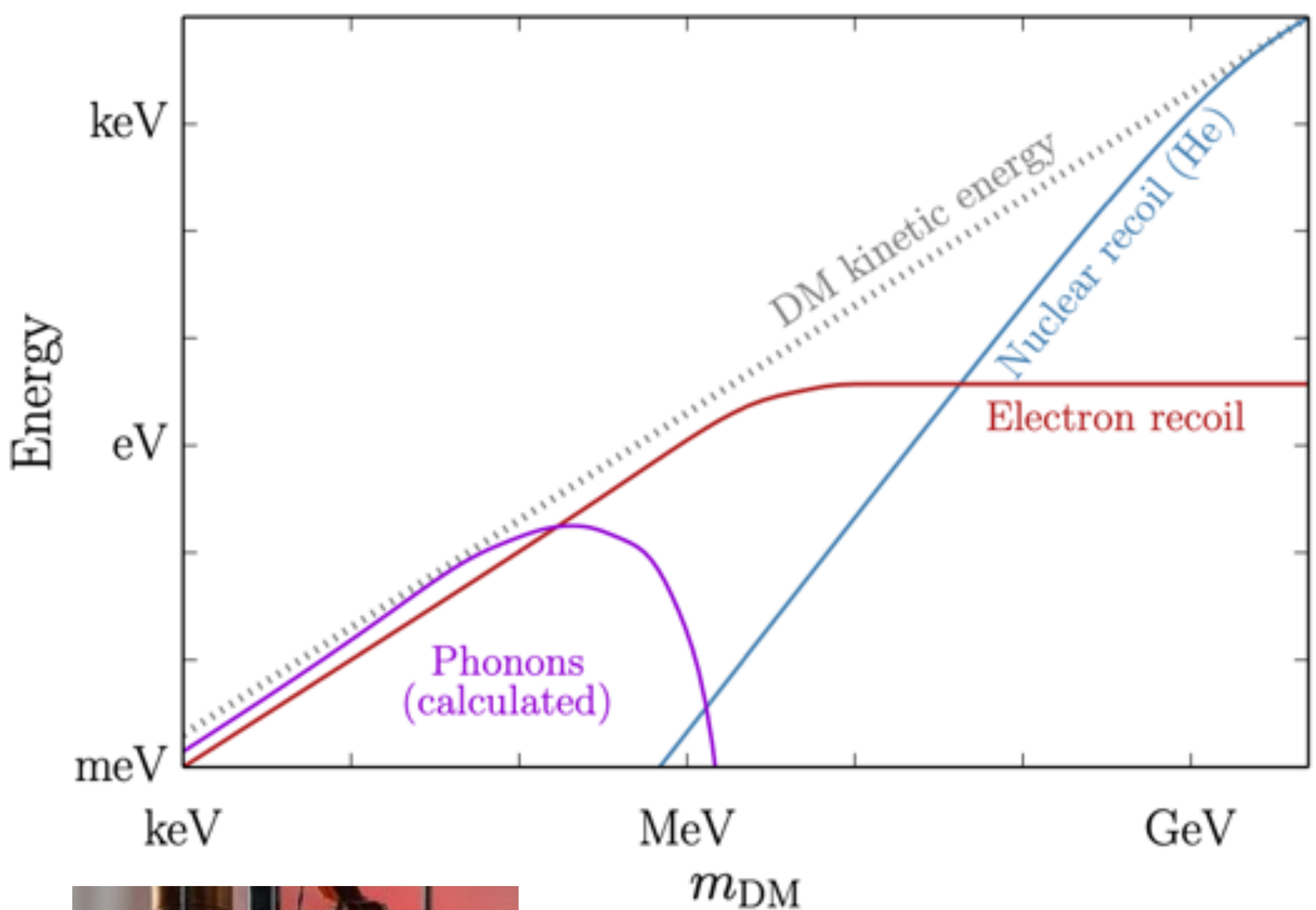

T. Lin, 2019

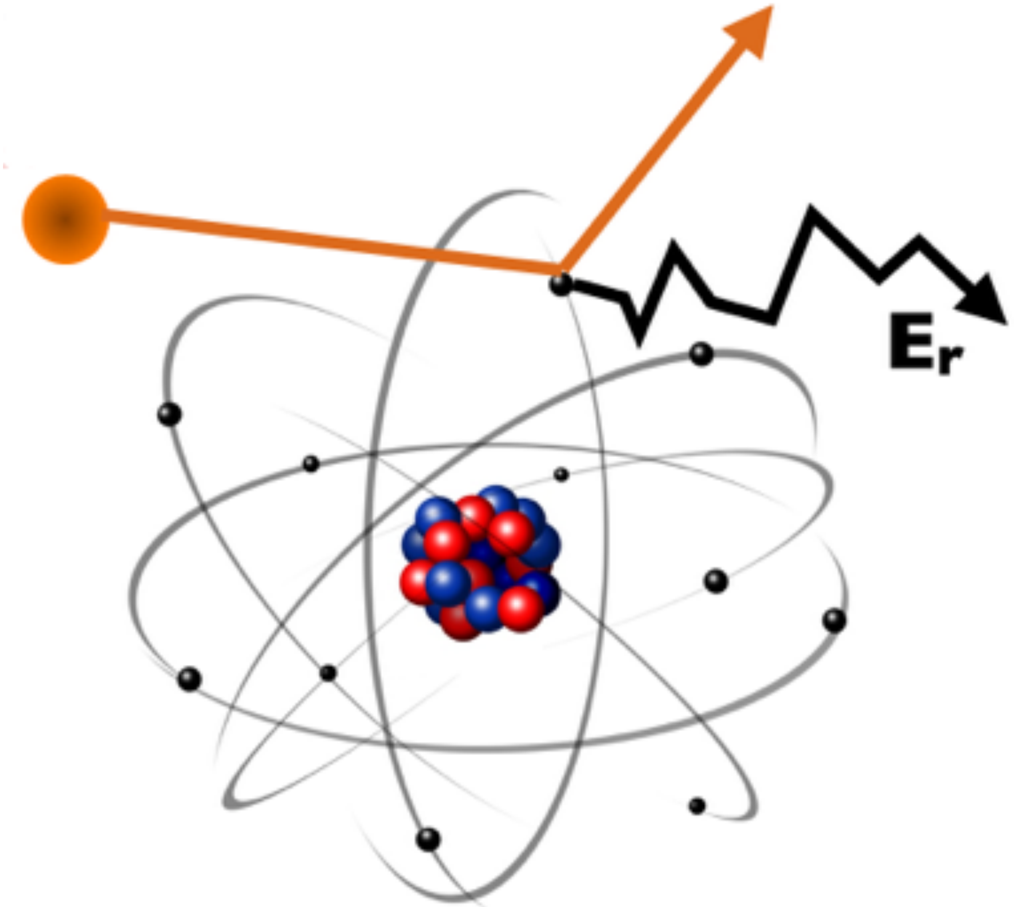

image credit: Carmen Carmona

Electron recoil

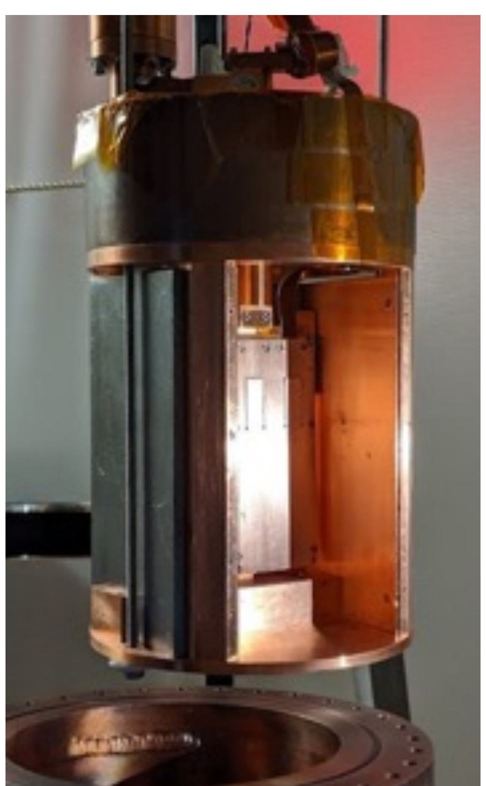

SENSEI collaboration

Cutting-edge technologies!

Thermal production of MeV DM is disallowed by BBN

light DM requires dark sectors

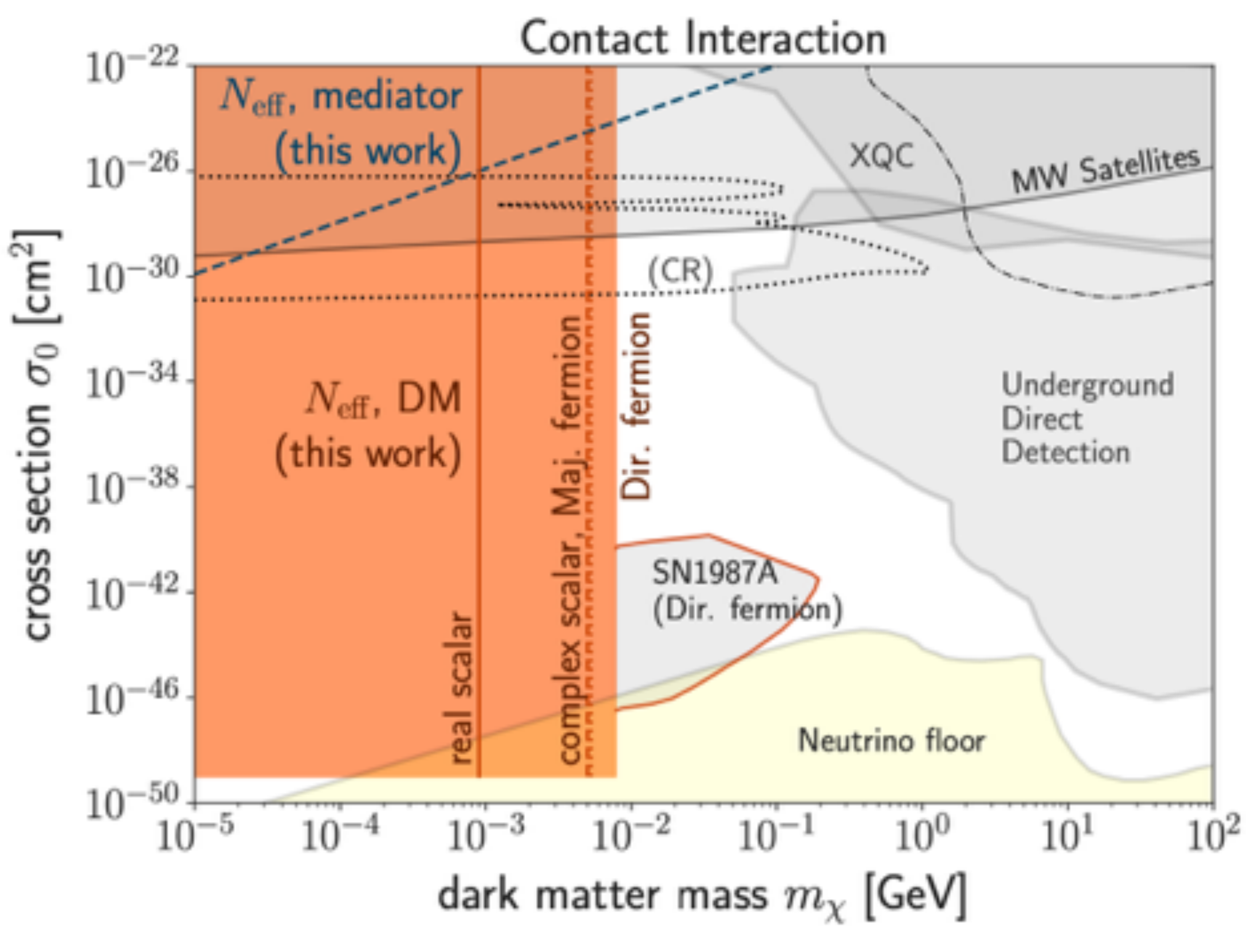

G. Krnjaic, S. D. McDermott, 2019

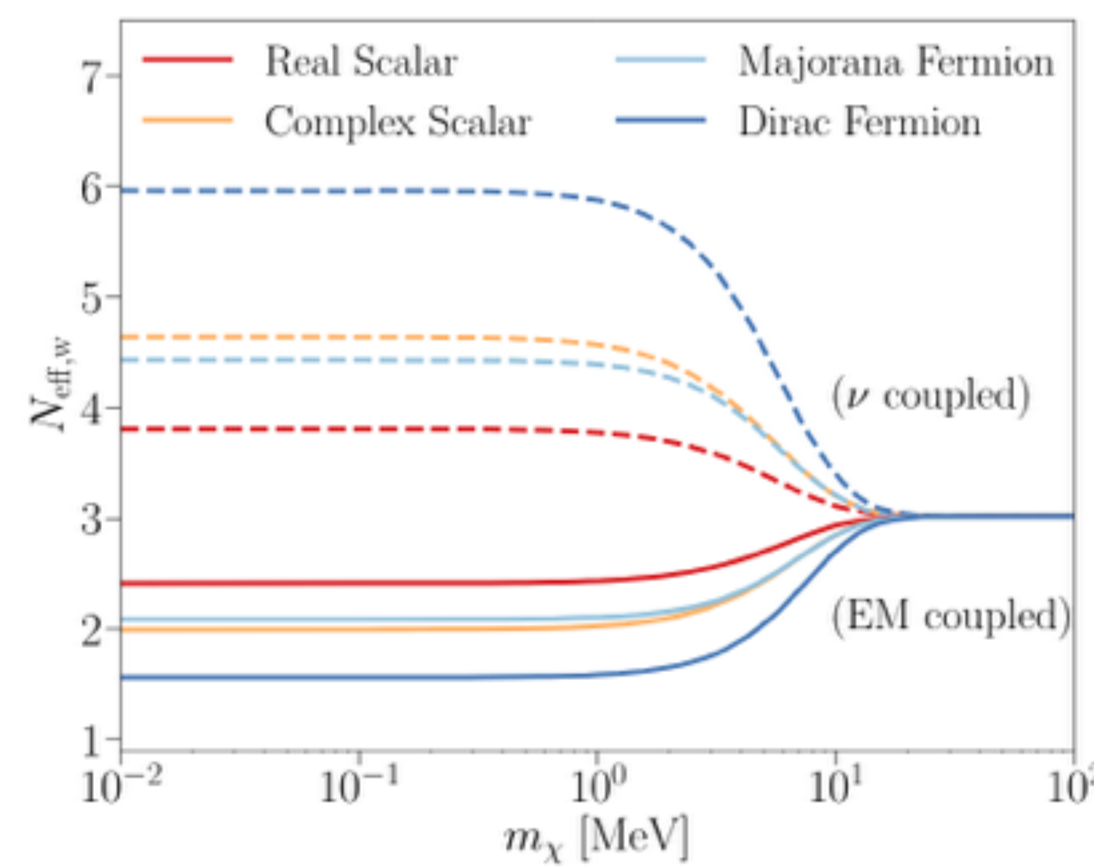

R. An, V. Gluscevic, E. Calabrese, J. C. Hill, 2022

Alternative: freeze-in!

Freeze-in:

the DM final abundance is built up gradually over time

$$\dot{n}_\chi + 3Hn_\chi = -\langle\sigma v\rangle \left(n_\chi^2 - n_{\chi,\mathrm{eq}}^2\right)$$

renormaizblae operators and **very small coupling**

$$\lambda \ll 1 \qquad Y_\chi \sim \lambda^2 \frac{m_{\mathrm{Pl}}}{T} \sim \lambda^2 \frac{m_{\mathrm{Pl}}}{m_\chi}$$

L. J. Hall, K. Jedamzik, J. March-Russell, S. M. West, 2009

IR freeze-in:

insensitive to temperatures above DM mass

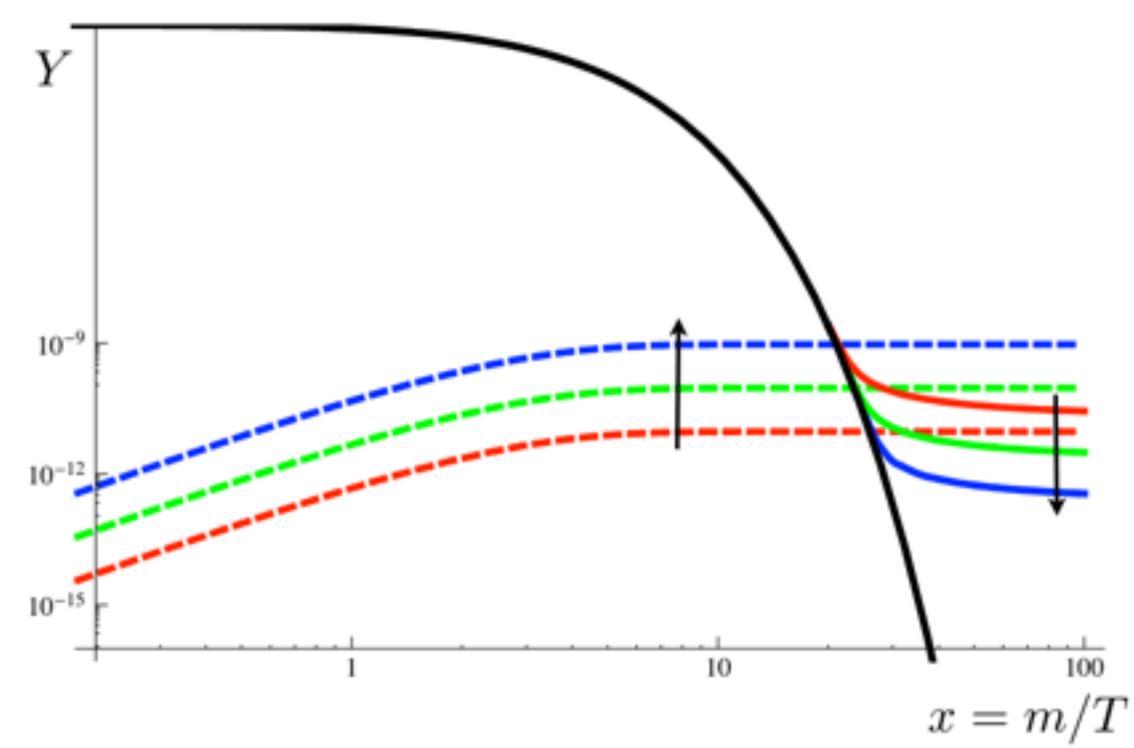

Benchmark freeze-in model:

$$\mathcal{L} \supset \frac{\epsilon}{2} F'_{\mu\nu} F^{\mu\nu}$$

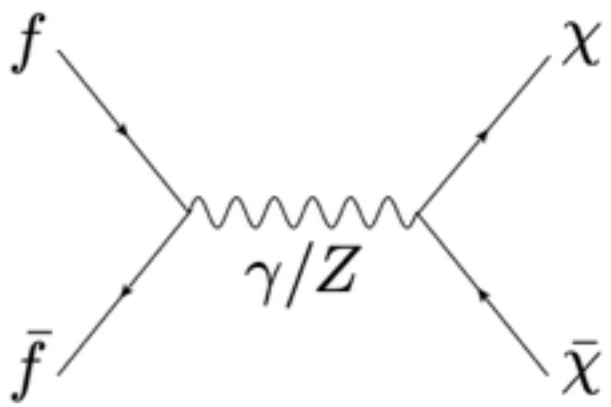

L. J. Hall, K. Jedamzik, J. March-Russell, S. M. West, 2009

X. Chu, T. Hambye, M. H. G. Tytgat, 2012

R. Essig, J. Mardon, T. Volansky, 2012

Freeze-in model:
extraordinarily **small coupling** between the DM and the SM.

Despite this, **the ultralight mediator** leads to a large enhancement of the direct detection cross section at low momentum transfers.

target of direct detection program!

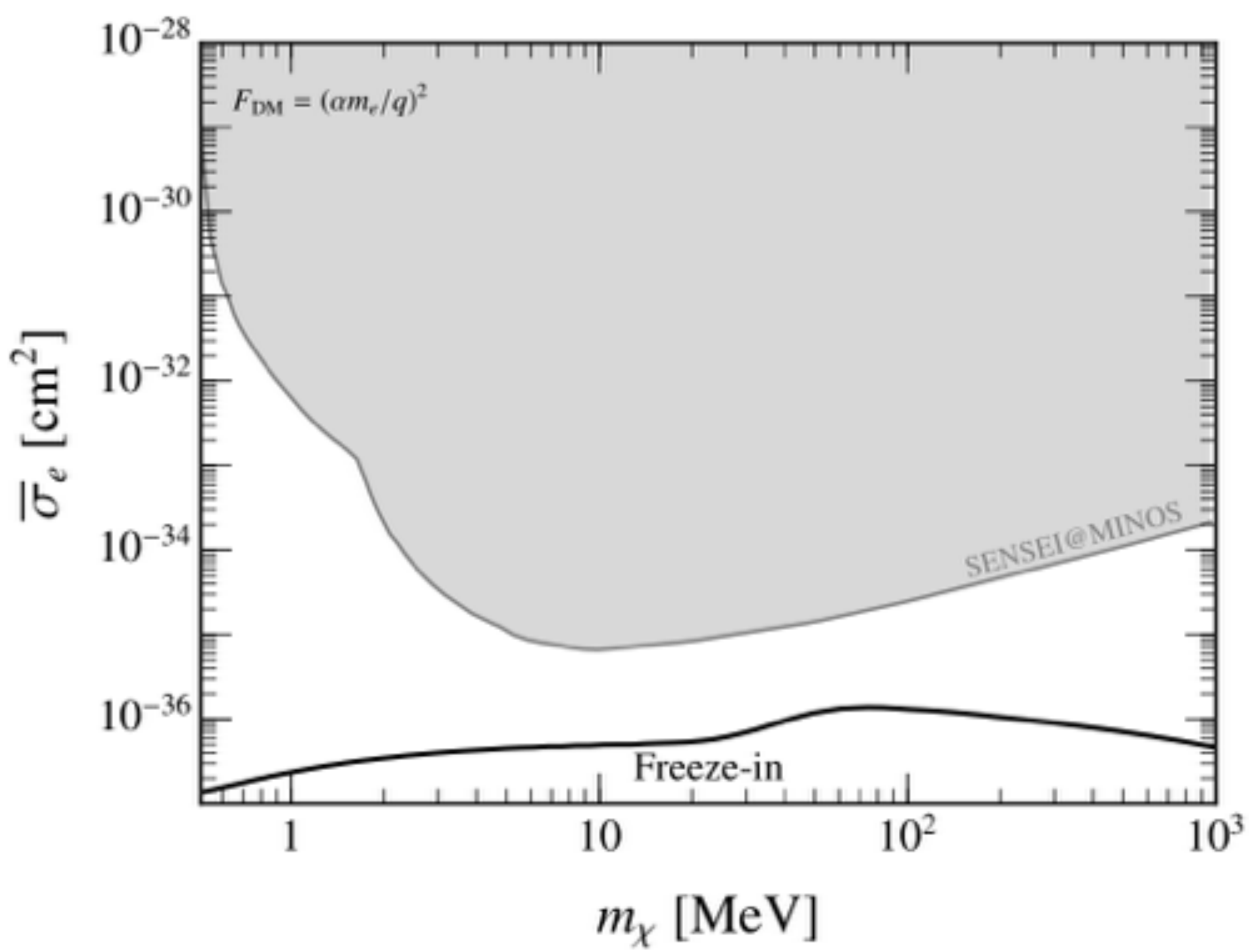

Relic abundance:

$$\dot{n}_\chi + 3Hn_\chi = \sum_B \langle \sigma_{B\overline{B}\to\chi\overline{\chi}} v\rangle (n_\chi^{\rm eq})^2$$

$$Y_\chi(x) = \int_{x_{\rm rh}}^{x} dx' \frac{s}{Hx'} \left[\sum_B \langle \sigma_{B\overline{B}\to\chi\overline{\chi}} v\rangle (Y_\chi^{\rm eq})^2 \right]$$

$$x \equiv m_\chi / T$$

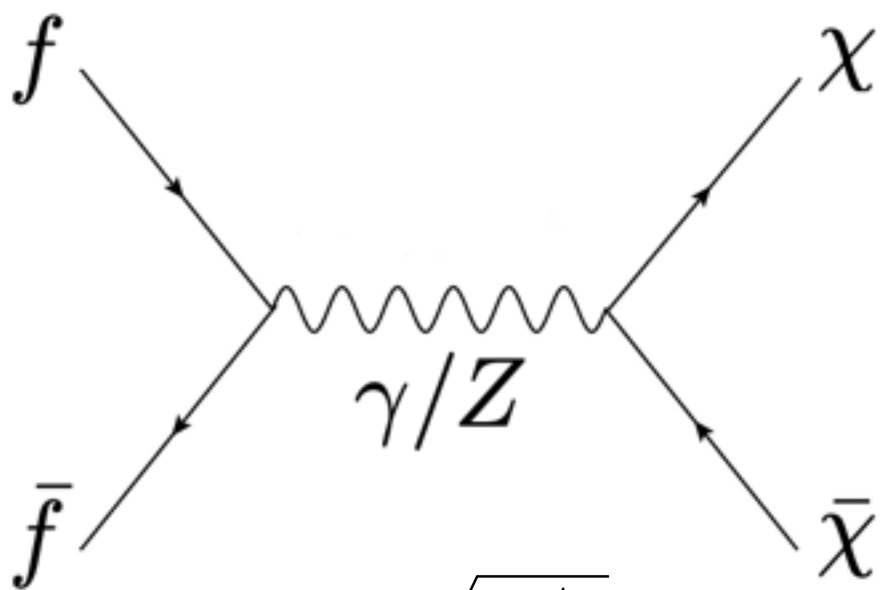

$$\kappa \equiv \epsilon\sqrt{\alpha'/\alpha}$$

Previous studies:

$$T_{\rm rh} >> m_\chi : \; x_{\rm rh} = 0$$

$$\text{fixed}\, m_\chi : \;\; \Omega_\chi = \Omega_{\rm CDM}$$

$$\to \text{unique}\, \kappa(m_\chi) \to \text{unique}\, \bar{\sigma}_e(m_\chi)$$

$$\overline{\sigma}_e = \frac{16\pi\mu_{\chi e}^2 \alpha^2 \kappa^2}{(\alpha m_e)^4}$$

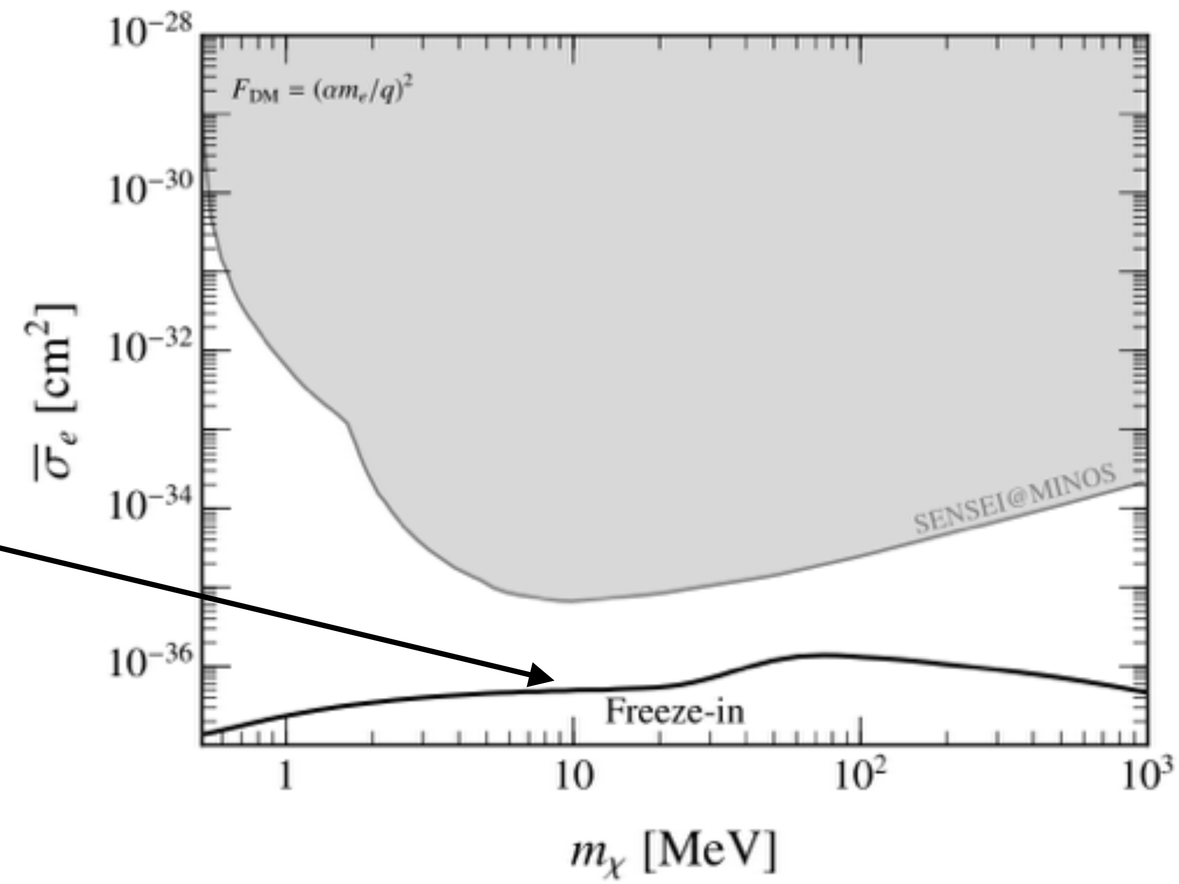

but reheating temperature can be below the mass!

Impact of reheating temperature:

$$5\,\mathrm{MeV} \lesssim T_{\mathrm{rh}} \ll m_\chi$$

$$\Gamma_{\mathrm{production}} \sim e^{-2m_\chi/T}$$

V. A. Kuzmin, V. A. Rubakov, 1998

C. Cosme, F. Costa, O. Lebedev, 2023

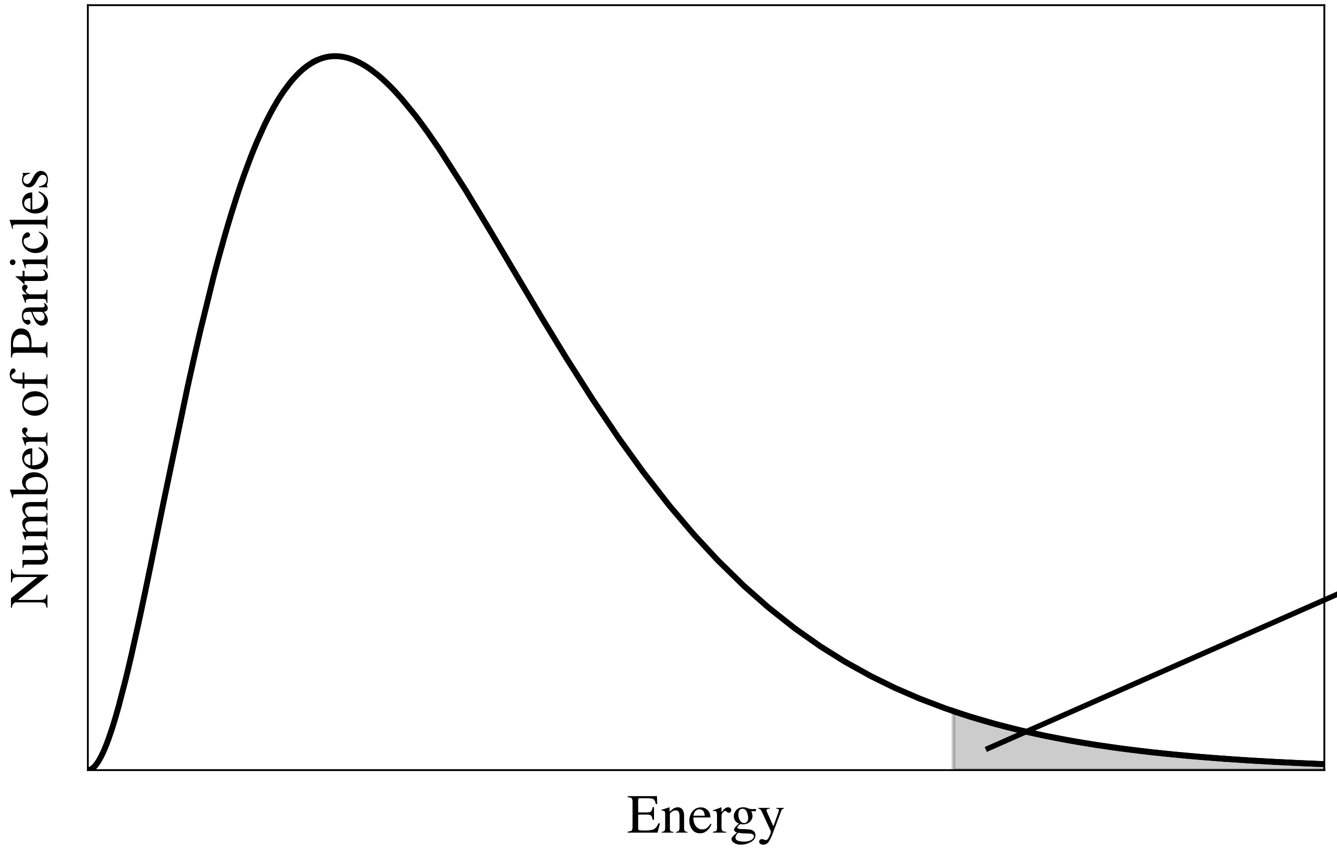

$$Y_\chi(x) = \int_{x_{\mathrm{rh}}}^{x} dx' \frac{s}{Hx'} \left[\sum_B \langle \sigma_{B\overline{B}\to\chi\overline{\chi}} v \rangle (Y_\chi^{\mathrm{eq}})^2 \right]$$

to match the relic abundance:
larger portal coupling, larger scattering cross-section!

Impact of reheating temperature on freeze-in benchmark:

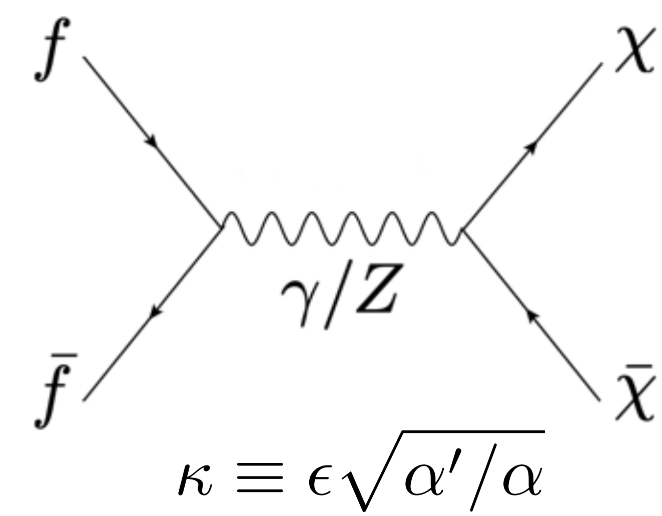

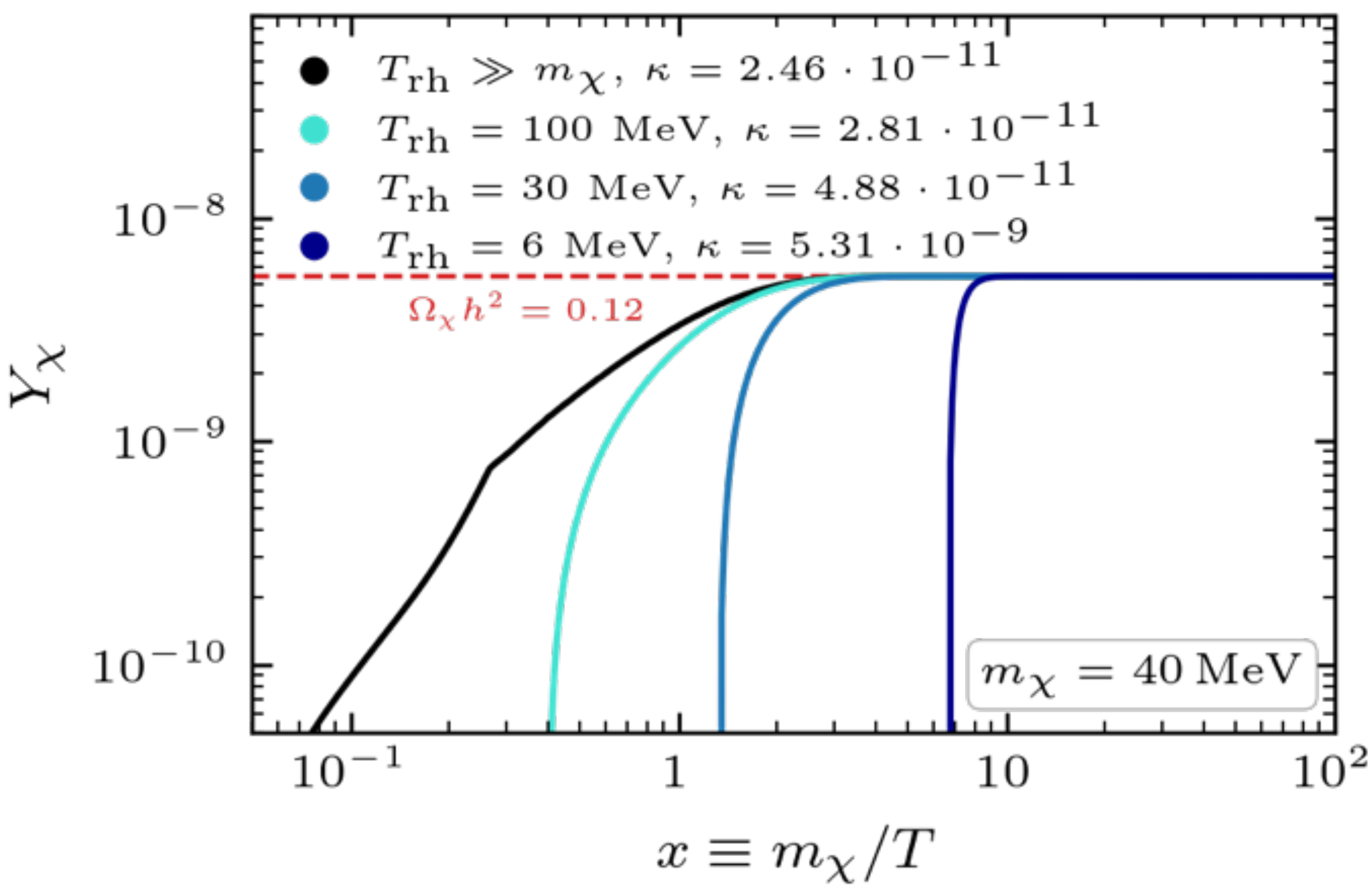

Low reheating temperature: Implications for direct detection

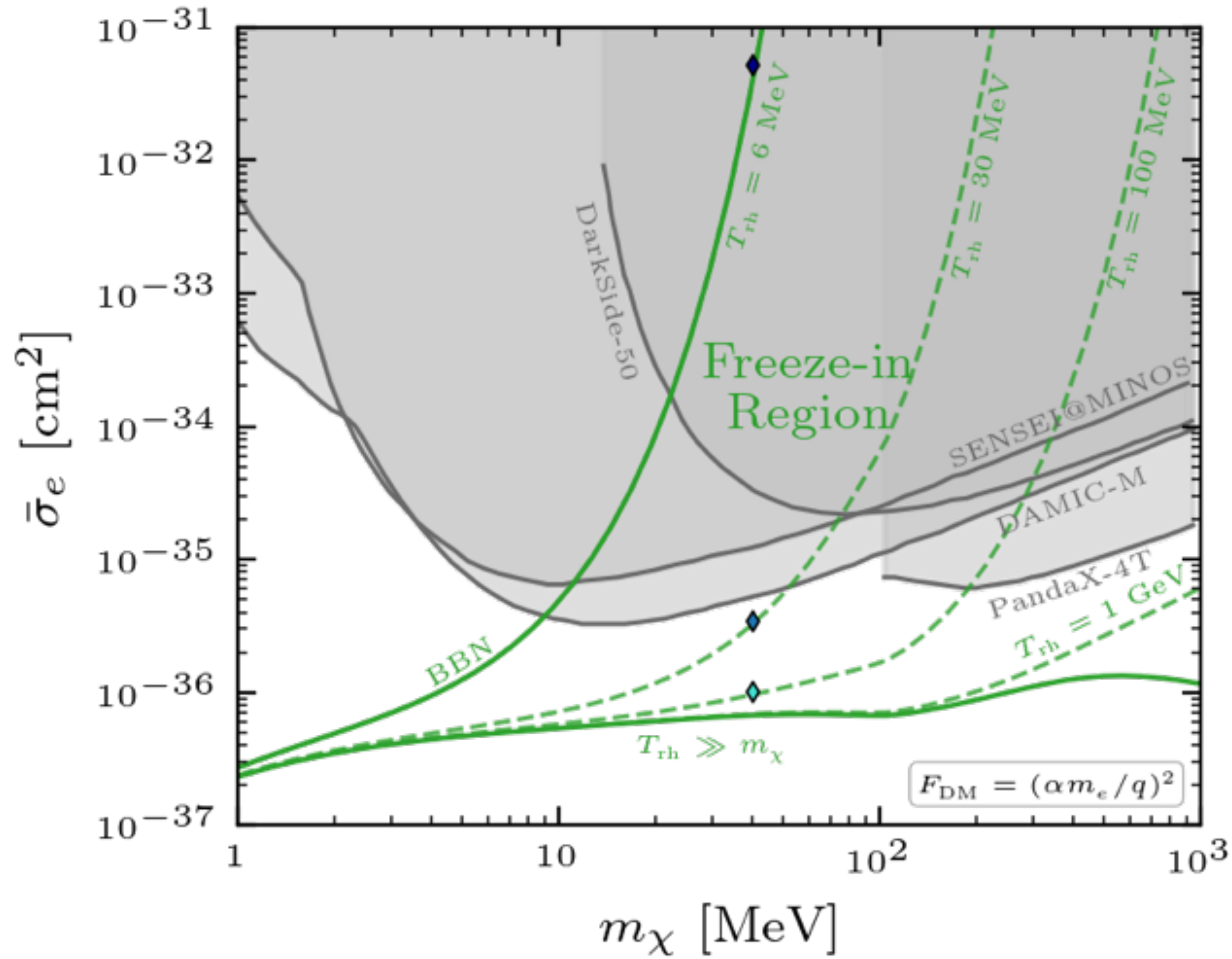

$$\frac{\kappa(T_{\rm rh} \ll m_\chi)}{\kappa(T_{\rm rh} \gg m_\chi)} \sim \sqrt{x_{\rm rh}}\, e^{x_{\rm rh}}$$

Freeze-in benchmark target:
a region defined by reheating temperature rather than a single curve.

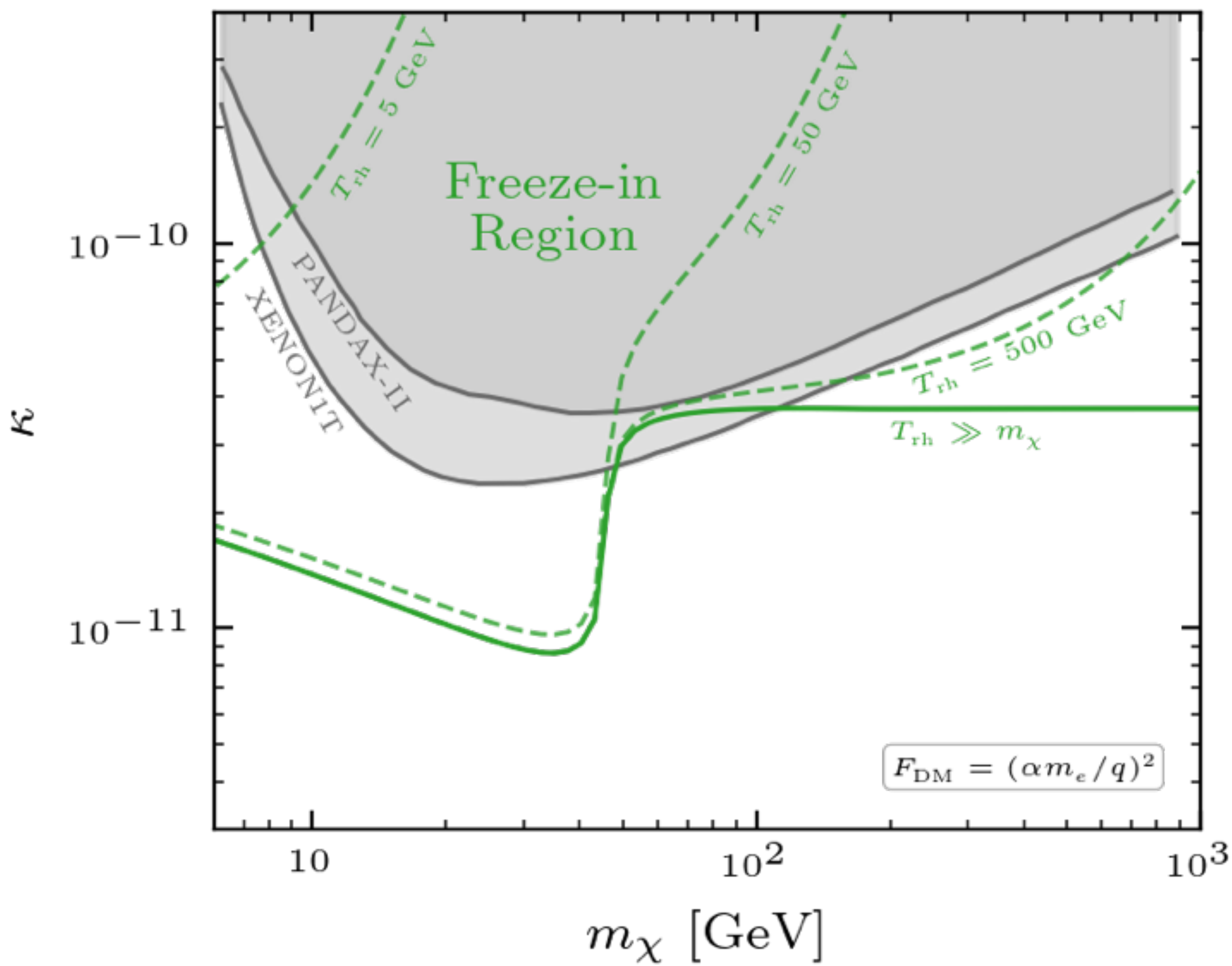
Freeze-in Region
PANDAX-II
XENON1T
$T_{rh} = 5$ GeV
$T_{rh} = 50$ GeV
$T_{rh} = 500$ GeV
$T_{rh} \gg m_\chi$
$F_{DM} = (\alpha m_e/q)^2$
κ
10^{-10}
10^{-11}
10
10^2
10^3
m_χ [GeV]

Alternative:

Opening up the parameter space
with high reheating temperature:

more complicated dark sectors that
introduce new dark degrees of freedom.

P. N. Bhattiprolu, R. McGehee, A. Pierce, 2023

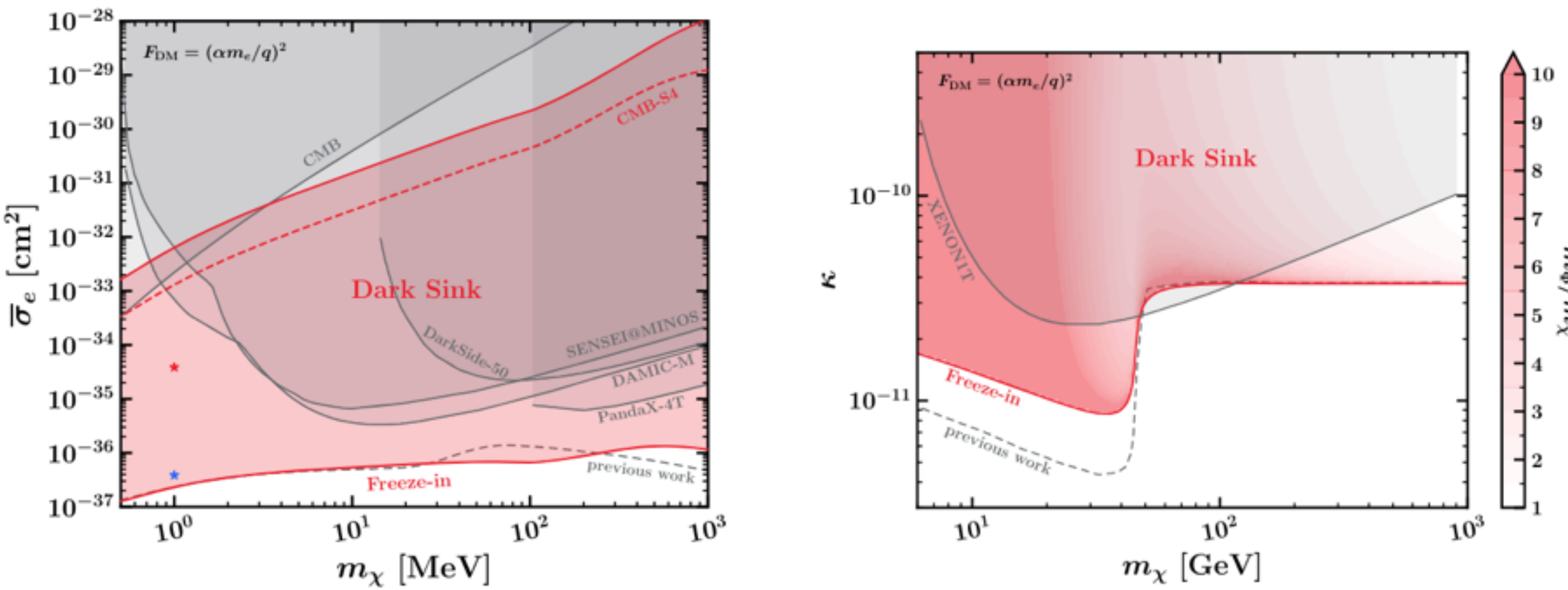

Maximum temperature of the Universe:

Reheating

(entropy production)

Radiation Domination

(entropy conservation)

t

$T \sim a^{-1}$

$T_{\rm rh}$

$\rho_{\rm rad}/\rho_{\rm tot} \ll 1$

$T \not\sim a^{-1}$

$T < T_{\rm max}$

Maximum temperature vs. reheating temperature:

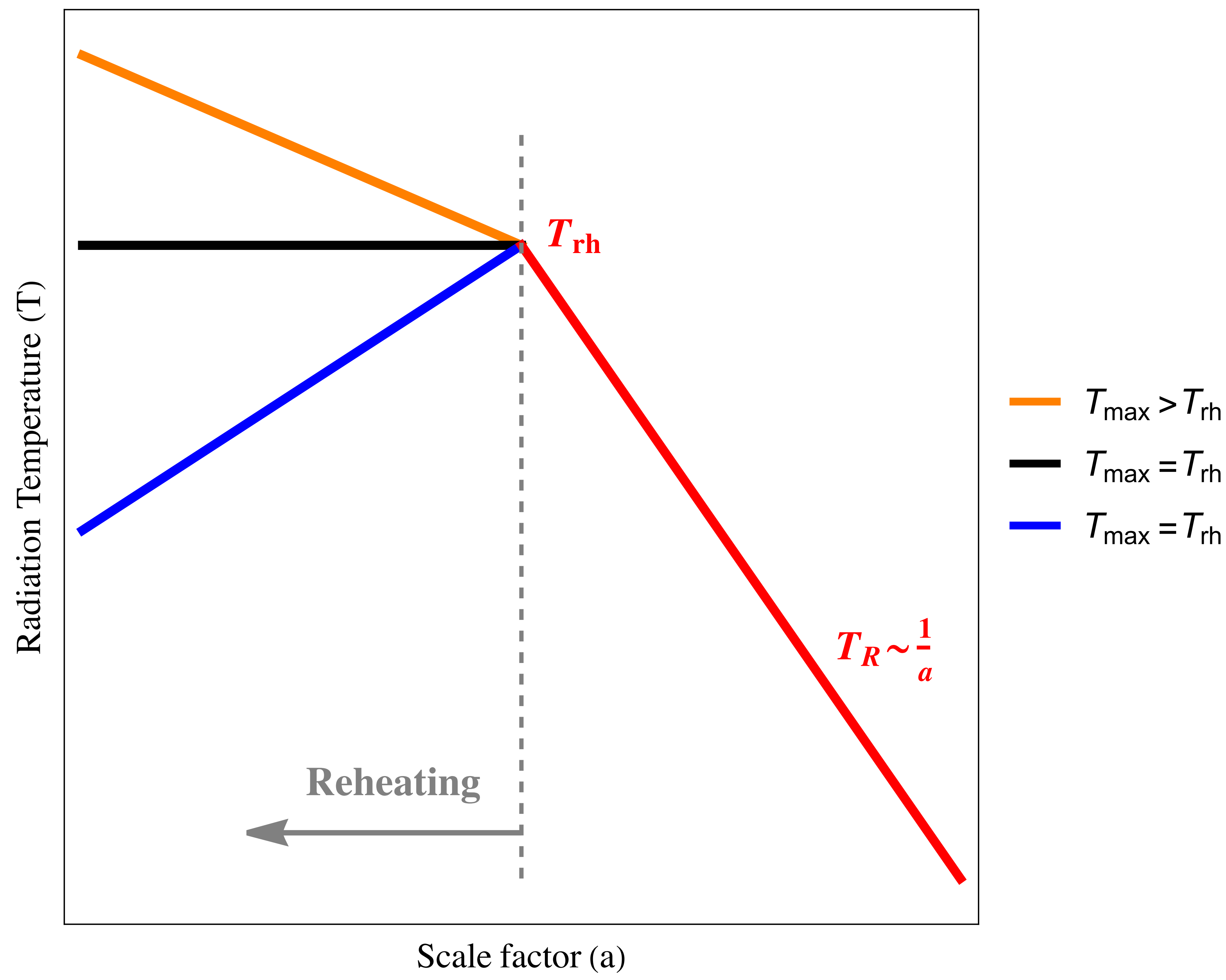

inflaton decays to radiation directly

D.J. H. Chung, E. W. Kolb, A. Riotto, 1998

G. F. Giudice, E. W. Kolb, A. Riotto, 2000

E. W. Kolb, A. Notari, A. Riotto, 2003

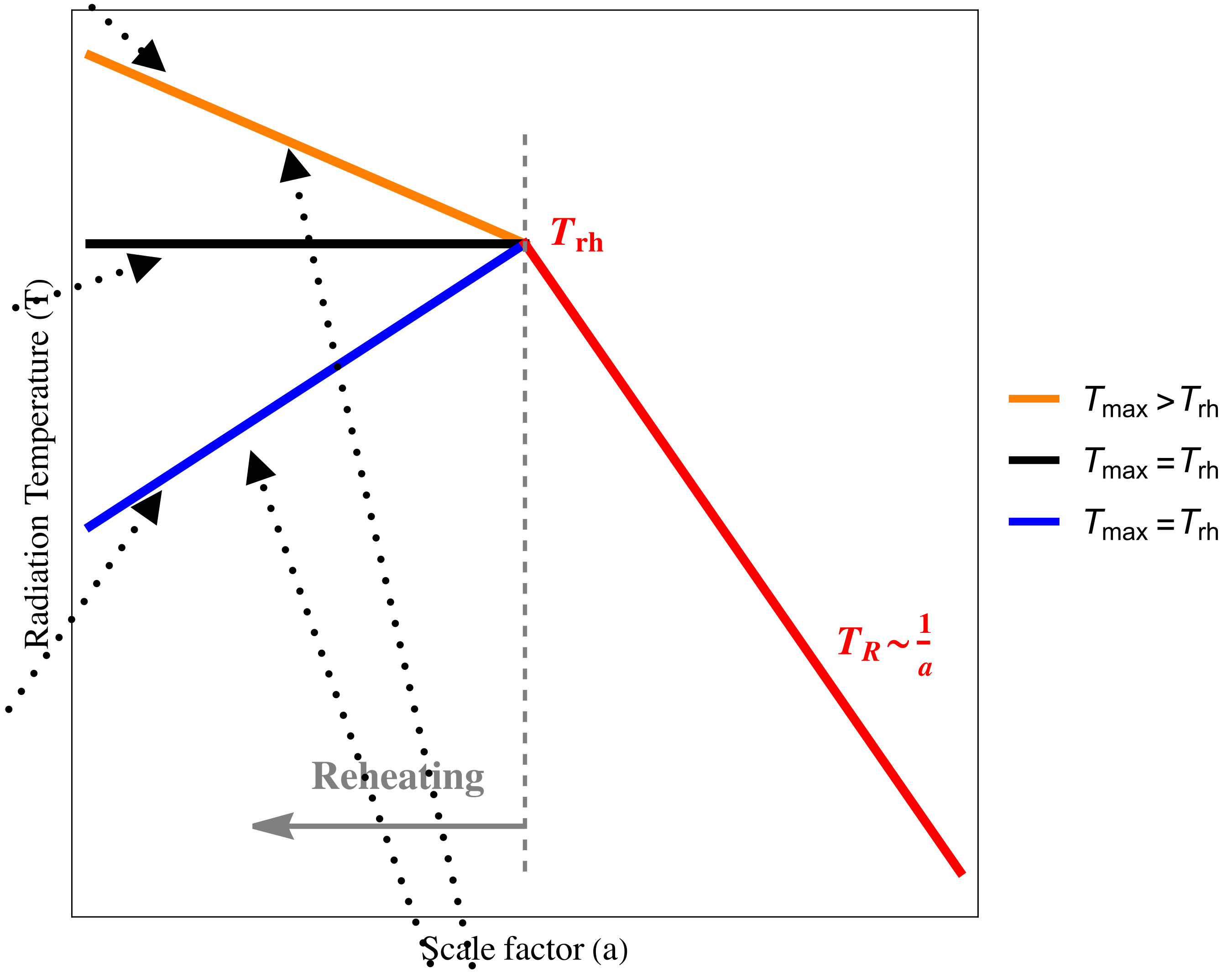

inflaton decays to an unstable particle which then decays to radiation

C. Cosme, F. Costa, O. Lebedev, 2024

inflaton has generic dissipation rate dependent on temperature and scale factor

R. T. Co, E. Gonzalez, K. Harigaya, 2021

Resonant reheating: s-channel inflaton annihilation

B. Barman, N. Bernal, Y. Xu, 2024

Conclusion:

The impact of the reheating temperature on the benchmark freeze-in model.

A reheating temperature below the mass of DM suppresses production rate; a larger portal coupling is required to achieve the observed relic abundance. This enhancement consequently lifts up the freeze-in benchmark target for direct detection.

A potential future detection that lies between the current observational limits and the traditional freeze-in benchmark would directly probe the reheating temperature and the conditions of the universe in its earliest moments.

DM-electron scattering rate

particle physics

$$\frac{\mathrm{d}\langle\sigma v\rangle}{\mathrm{d}\ln E_R} = \frac{\overline{\sigma}_e}{8\mu_{\chi e}^2}\int q\ \mathrm{d}q|f(k,q)|^2|F_{DM}(q)|^2\eta(v_{min})$$

$$\overline{\sigma}_e = \frac{\mu_{\chi e}^2}{16\pi m_\chi^2 m_e^2}\overline{|\mathcal{M}_{\chi e}(q)|}^2_{q^2=\alpha^2 m_e^2}$$

$$F_{DM}(q) \simeq \begin{cases} 1 & \textbf{heavy mediator} \\ \frac{\alpha m_e}{q} & \textit{electric dipole moment} \\ \frac{\alpha^2 m_e^2}{q^2} & \textbf{light mediator} \end{cases}$$

$$\mathcal{L} \supset -\frac{1}{4}\hat{X}_{\mu\nu}\hat{X}^{\mu\nu} + \frac{\epsilon_Y}{2}\hat{X}_{\mu\nu}\hat{B}^{\mu\nu} - e'\hat{X}_\mu\overline{\chi}\gamma^\mu\chi.$$

$$\hat{Z}_\mu = Z_\mu$$
$$\hat{A}_\mu = A_\mu + \epsilon A'_\mu$$
$$\hat{X}_\mu = A'_\mu - \epsilon \tan\theta_W Z_\mu.$$

$$\epsilon \equiv \epsilon_Y \cos\theta_W$$

$$\begin{aligned}\mathcal{L} \supset &- \epsilon e A'_\mu J^\mu_{\mathrm{EM}} - e' J^\mu_{\mathrm{DM}}\left(A'_\mu - \epsilon\tan\theta_W Z_\mu\right) \\ &+ i\epsilon e\left[F'^{\mu\nu}W^+_\mu W^-_\nu - \left(\partial_\mu W^+_\nu - \partial_\nu W^+_\mu\right)A'^\mu W^{-\nu}\right. \\ &+ \left.\left(\partial_\mu W^-_\nu - \partial_\nu W^-_\mu\right)A'^\mu W^{+\nu}\right].\end{aligned} \tag{S3}$$

$$\overline{|\mathcal{M}|}^2_{f\bar{f}\to\chi\bar{\chi}} = \frac{32}{3}\pi^2\alpha^2\kappa^2 N_f \left(s+2m_\chi^2\right)\left[\frac{Q_f^2}{s^2}\left(s+2m_f^2\right) - 2Q_f V_f \tan\theta_W \frac{\left(s+2m_f^2\right)\left(s-m_Z^2\right)}{s\left[\left(s-m_Z^2\right)^2+m_Z^2\Gamma_Z^2\right]} \right.$$
$$\left. + \tan^2\theta_W \frac{V_f^2\left(s+2m_f^2\right)+A_f^2\left(s-4m_f^2\right)}{\left(s-m_Z^2\right)^2+m_Z^2\Gamma_Z^2}\right], \tag{S4}$$

$$\overline{|\mathcal{M}|}^2_{\phi^+\phi^-\to\chi\bar{\chi}} = \frac{32}{3}\pi^2\alpha^2\kappa^2\left(1+\frac{2m_\chi^2}{s}\right)\left(1-\frac{4m_\phi^2}{s}\right), \tag{S5}$$

$$\overline{|\mathcal{M}|}^2_{W^+W^-\to\chi\bar{\chi}} = \frac{8}{27}\pi^2\alpha^2\kappa^2\left(\frac{m_Z}{m_W}\right)^4\frac{\left(s+2m_\chi^2\right)\left(s-4m_W^2\right)\left(s^2+20sm_W^2+12m_W^4\right)}{s^2\left[\left(s-m_Z^2\right)^2+m_Z^2\Gamma_Z^2\right]}, \tag{S6}$$